Journal of Ocean, Mechanical and Aerospace
-Science and Engineering-, Vol.49

November 30, 2017

Numerical Analysis of Resistance Acting on Sea-Going Pusher and Barge System

Masaaki Sano [a,*], Yusuke Kawano [b], Takuto Yamamoto [c] and Hironori Yasukawa [a]

[a)] *Graduate school of Engineering, Hiroshima University, Japan*
[b)] *Undergraduate student, Hiroshima University, Japan (at the time of this research)*
[c)] *1st grade of master's course student, Hiroshima University, Japan*

*Corresponding author: masaaki-sano@hiroshima-u.ac.jp

Paper History

Received: 12 - October - 2017
Received in revised form: 6-November-2017
Accepted: 30-November-2017

ABSTRACT

Because a pusher and barge system (P/B) can be divided into a pusher and a barge(s), the pusher does not need to wait for the completion of loading/unloading, and it can start a next voyage soon after arriving. Therefore, a good transportation efficiency can be expected. In these days, a P/B is also available to a sea-going service by developing a mechanical connection which enabled a P/B to achieve the seaworthy performance in waves. However, there is a concern that the navigation speed is usually less than same-size cargo ships. It may be due to significant vortices generated in the gap at the connection, but the mechanism is still unclear. From this viewpoint, in this study, CFD analysis was carried out to investigate the resistance performance associating with the flow and pressure fields around the pusher and barge, especially with focus on the gap between them. We discussed the unique change of the resistance characteristic depending on the barge load conditions.

KEY WORDS: *Pusher and barge system, Resistance, Load condition, CFD*

NOMENCLATURE

L_{WL}	Ship length between perpendiculars
L_{WL}	Ship length waterline
B	Ship breadth
d	Ship draft
WSA	Wetted surface area
∇	Displacement
F_n	Froude number
V	Flow velocity
U_0	Ship velocity
C_P	Pressure coefficient
ΔX_F	Longitudinal force component due to friction
ΔX_P	Longitudinal force component due to pressure

1.0 INTRODUCTION

1.1 Sea-going pusher and barge system

A pusher and barge system (P/B) originally has been developed in a river and an inland waterway where single barge or multiple barges coupled together are pushed by a powerful pusher boat. Because a P/B is able to carry a large amount of cargos compared to rail cars or trucks, it has an economic and environmental efficiency [1].

There have been a lot of studies about its performance so far. For example, Yasukawa et al. [2] investigated the hydrodynamic force characteristics of 9 coupled barges through the towing tank tests. Based on their data, Koh et al. [3] ran the maneuvering simulation, and Hamaguchi et al. [4] studied the maneuverability in a uniform river flow based on the simulation. The shallow water effect on the maneuverability of a P/B was also investigated by e.g. Maimun et al [5]. Meanwhile, Sano and Hasegawa [6] tried to tackle with a more specific case. They discussed the maneuvering motions of a tug-barge system (T/B) and a P/B sailing in the Mahakam River in Indonesia. It was a rudimentary study to investigate the possibility of introducing a P/B for coal transport in that river instead of a T/B.

By contrast to popularity of such a P/B in river service, a sea-going P/B has not been positively developed so far. Because a

JOMAse | Received: 12-October-2017 | Accepted: 30-November-2017 | [(49) 1: 1-7]
Published by International Society of Ocean, Mechanical and Aerospace Scientists and Engineers, www.isomase.org., ISSN: 2354-7065 & e-ISSN: 2527-6085

seaworthy performance was required, the rope connection, which was usually used for a river-going P/B, was not enough strong to connect the pusher and barge in waves. This problem was solved by developing a mechanical connection system [7][8]. However, there is another concern that a P/B has to compete with normal cargo ships at sea and its navigation speed is usually less than cargo ships. It may be due to significant vortices generated in the gap between the pusher and barge, but there seems no data to clearly discuss the mechanism so far.

From this viewpoint, in this study, CFD analysis is carried out to understand the resistance characteristics through the analysis of the flow and pressure fields around the pusher and barge, especially focusing on the gap between them. Since the step appears or disappears around the pusher-barge connection depending on the barge load condition, both full-load and ballast conditions are considered. The results could provide good knowledge for the hull design of a sea-going P/B expecting smaller resistance in future.

1.2 Availability in Indonesia

Indonesia consists of a lot of islands and the marine transportation network has been developed (Figure 1). Since these islands are nearly located each other, a ship do not need a long voyage among them and only a few days are usually required for each voyage. Therefore, the frequency of port calls tends to increase which means the waiting time while loading/unloading frequently occurs. Such a situation in Indonesia would be preferable for the activity of a sea-going P/B [9]. Because a P/B can be divided into a pusher and a barge, the pusher does not need to wait for completion of loading/unloading, and it can start a next voyage soon after arriving. Therefore, we could expect to improve the transportation efficiency by saving the waiting time and transferring that time to the next voyage time. Furthermore, since a larger number of unmanned barges can be operated by a smaller number of manned pushers, it would bring about a great saving of the building cost and manning cost [8]. In particular, when the volume of cargoes increases in near future, this advantage could become critically important.

The flexible availability of a P/B is also considered as one of good advantages. For example, because one pusher can be coupled with any types of the barge, a P/B could transport a variety kinds of cargoes just by changing the type of the barge. As another example, when it tries to access to an undeveloped port or river upstream which are not dredged enough for deep-draft vessels, a P/B has an option to select a shallow draft barge and can access there.

Figure 1: Map of Indonesia
(from SekaiChizu: http://www.sekaichizu.jp/)

2.0 SUBJECT SEA-GOING P/B

Compared to a river-going P/B, a sea-going P/B usually does not make a barge convoy and it is a common style in which one pusher pushes one barge. In order to make the navigation speed faster, the bow shape of the barge is designed like a normal ship, and the pusher fits in the recess part named as a notch manufactured in the stern of the barge.

The principal dimension of the sea-going P/B is listed in Table 1. The length waterline of the pusher is 34 m, that of the barge is 119 m and that of the P/B is 141.6 m which is shorter than the sum of the length of the pusher and barge because the pusher is put into the notch. Two load conditions of the barge were considered; full-load condition and ballast condition whose draft is about 58 % of the full-load one. Now we have the plan to build a 1/40 scale model of the P/B, the same scale model of the P/B was considered for CFD analysis in this study. Figure 2 shows the side view of the P/B under each load condition.

Table 1: Principal dimension of the real scale P/B

Item		Pusher	Barge		P/B	
		-	Full	Ballast	Full	Ballast
L_{PP}	m	31.6	119.0		-	
L_{WL}	m	34.0	119.0		141.6	
B	m	13.0	24.0		24.0	
d	m	5.8	8.2	4.75	8.2	5.8
WSA	m^2	756.5	4251.9	3338.6	5008.4	4095.1
V	m^3	1570.2	19100.3	10672.0	20670.5	12242.2

Figure 2: Overview of the pusher and the full-load barge (above) and the ballast barge (below)

3.0 OUTLINE OF NUMERICAL CALCULATION

The hydrodynamic force acting on the bare hull of the P/B in straight running was calculated by CFD. The steady-state solver for incompressible, turbulent flow supplied with OpenFOAM [10] ver.2.3.0 was chosen for this purpose. Spalart-Allamaras model was used for the turbulence model. As mentioned above, the 1/40 scale model of the P/B was considered as the target in this study.

There is a well-known three dimensional extrapolation method for ship resistance analysis. It assumes that the total resistance can be calculated by linear summation of three components: viscous friction resistance, viscous pressure resistance and wave-making resistance. Considering the aim of this study was to evaluate the change of the viscous resistance depending on the load condition, the free surface was considered to be rigid in order to simplify the problem. Thus, CFD was calculated at the P/B's L_{WL}-based Froude number F_n=0.1.

JOMAse | Received: 12-October-2017 | Accepted: 30-November-2017 | [(49) 1: 1-7]
Published by International Society of Ocean, Mechanical and Aerospace Scientists and Engineers, www.isomase.org., ISSN: 2354-7065 & e-ISSN: 2527-6085

O-xyz was defined at the right hand side coordinate system where the AP of the pusher was set at x=0 in the longitudinal direction, the center-plane was placed at y=0 in the lateral direction and the water surface was at z=0 in the vertical direction. Because the hull is left-right symmetrical with respect to the center plane, only the left domain was selected for computation: $|x/L_{WL}|<2.52$, $0<y/L_{WL}<1.26$, $0<z/L_{WL}<0.7$ and subdivided into about 400~500 million cells for the P/B. Especially, the domain near the hull body was subdivided into more number of cells.

4.0 RESULT AND DISCUSSION

4.1 Interaction between the pusher and barge

Because the pusher is positioned behind the barge, the pusher is exposed to the significant wake of the barge. Meanwhile, the flow pressure spread over the pusher bow influences the pressure field around the barge stern. This is an interaction between the pusher and barge, and considered as a unique characteristic of the P/B. In order to find out such an interaction, we tried to calculate the resistance not only of the P/B, but also the pusher without the barge (P) and the barge without the pusher (B). Figure 3 (Full-load) and Figure 4 (Ballast) show the resistance of (a) P, (b) B, (c) P+B, and (d) P/B. The components of the "Total" resistance, i.e., "Pressure (viscous pressure resistance)" and "Friction (viscous friction resistance)" are also presented. Comparing (c) and (d), we can see the interaction between them.

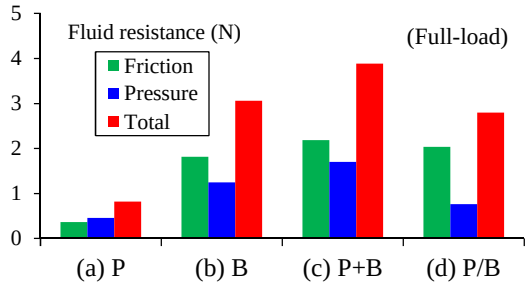

Figure 3: Comparison of the resistance among a variety of configurations (Full-load)

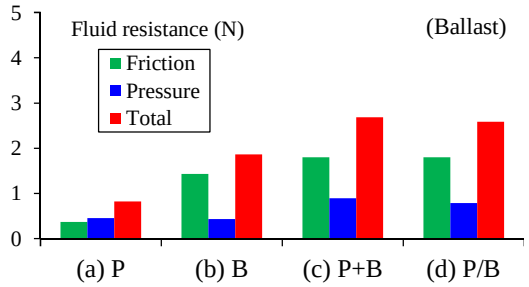

Figure 4: Comparison of the resistance among a variety of configurations (Ballast)

The total resistance of (d) P/B is smaller than that of (c) P+B by 27.9 (%) in the full-load condition, and 3.8 (%) in the ballast condition. We see this reduction results mainly from the reduction of the pressure resistance; the reduction rate is 55.1 (%) and 12.1 (%) in the full-load and ballast conditions respectively. As a conclusion here, the interaction between the pusher and barge is significantly large when the pusher pushes the full load barge, and it becomes small as the amount of load (barge draft) decreases.

4.2 Resistance characteristic of the P/B

4.2.1 Resistance acting on the pusher and barge of the P/B

The resistance of the P/B is defined as the sum of the resistance acting on the pusher and that on the barge. Figure 5 (Full-load) and Figure 6 (Ballast) show each resistance component acting on these parts of the P/B.

Comparing the total resistance of "P/B" between different barge load conditions, the difference of the percentage is only 8.1 %. However, the amount of each resistance component acting on each pusher and barge is quite different according to the barge load conditions. For example, the pressure resistance of the ballast barge pushed by the pusher is negative (ref: blue bar of "B of P/B" in Fig.6), which means the barge is subjected to a propulsive force, and its amount is much larger than the full load barge (ref: blue bar of "B of P/B" in Fig.5). Meanwhile, the larger pressure resistance acts on the pusher when pushing the ballast barge (ref: blue bar of "P of P/B" in Fig.6) than when pushing the full-load barge (ref: blue bar of "P of P/B" in Fig.5).

With focus on the friction resistance which is supposed to be proportional to the wetted surface area, that of the full-load barge is surely larger than the ballast barge (ref: green bar of "B of P/B" in Fig.5 vs. Fig.6). On the other hand, the friction resistance of the pusher when pushing the full-load barge is smaller than when pushing the ballast barge despite the wetted surface area of the pusher is constant (ref: green bar of "P of P/B" in Fig.5 vs. Fig.6).

Such unique characteristics of the resistance of the P/B result from the change of the strength of the interaction between the pusher and barge depending on the barge load conditions. Their mechanisms are discussed in detail in following sections.

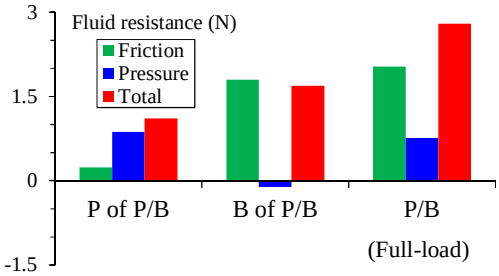

Figure 5: Breakdown of resistance components acting on each pusher and barge of the P/B (Full-load)

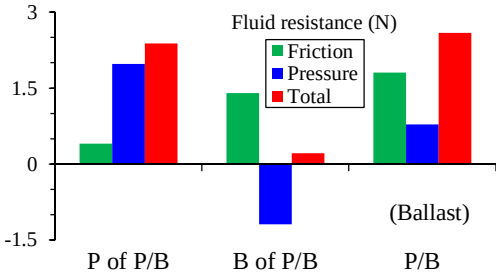

Figure 6: Breakdown of resistance components acting on each pusher and barge of the P/B (Ballast)

JOMAse | Received: 12-October-2017 | Accepted: 30-November-2017 | [(49) 1: 1-7]
Published by International Society of Ocean, Mechanical and Aerospace Scientists and Engineers, www.isomase.org., ISSN: 2354-7065 & e-ISSN: 2527-6085

4.2.2 Friction resistance and its mechanism

Figure 7 shows the color contour map of the flow velocity around the hull, which is nondimensionalized by the ship speed i.e. $|V|/U_0$. The focus is given on the connection in Figure 8. The distribution of the friction force component i.e. ΔX_F in the longitudinal direction is also presented in Figure 9 where the horizontal axis (x) is nondimensionalized by the length of the pusher waterline: $x'=x/L_{PP(\text{pusher})}$. Thus, $x'=1$ indicates the position of the pusher bow. Note the integral value of this plot line from the bow to the stern is equal to the friction resistance:

$$R_F = -\int \frac{dX_F}{dx} dx \quad (1)$$

From Figure 7, in the case of the P/B(Ballast), the flow along the shallow-draft barge is blocked by the deeper pusher bow, and it is accelerated again when going around the pusher bow. Meanwhile, the flow seems to be separated at the connection and stagnant in the large recess part in the case of the full-load barge. It causes to expose the pusher to the resultant significant wake.

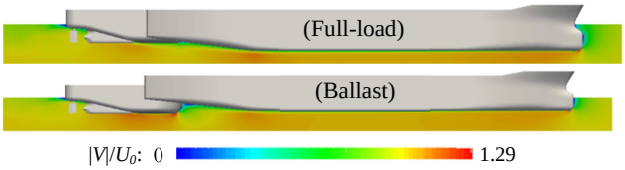

Figure 7: [Side view] Contours of the nondimensional flow velocity around the P/B (above: Full-load / below: Ballast)

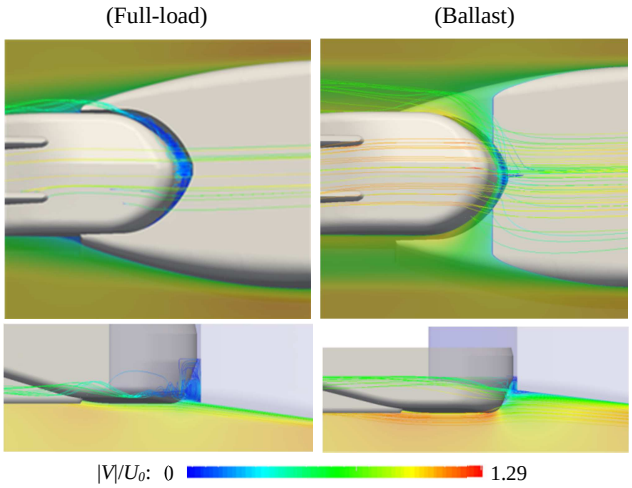

Figure 8: Enlarged side view of the contours of the non-dimensional flow velocity with stream lines at the connection (left: Full-load / right: Ballast)

The difference of the flow field around the connection results in the different distribution of the friction force component as shown in Figure 9. Since the wetted surface area of the full-load barge is larger than the ballast barge, we see the large friction resistance acts on the full load barge. On the other hand, it is noteworthy that the pusher, i.e. $x' < 1$, is subject to the lower resistance when pushing the full-load barge than the ballast barge. As observed in Figure 8, because the flow is accelerated at the bow of the pusher behind the ballast barge, it causes the high velocity gradient there, and results in the increase of the friction resistance of the pusher. In contrast, the significant wake shed from the full-load barge changes the velocity gradient around the pusher to be mild. We guess it contributes to reduce the friction resistance of the pusher behind the full-load barge.

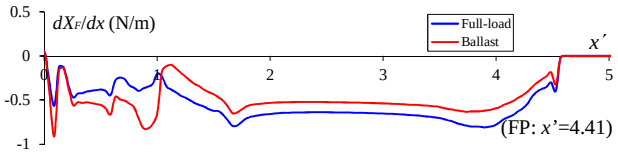

Figure 9: Longitudinal distribution of the friction force component

4.2.3 Pressure resistance and its mechanism

Figure 10 shows the color contour map of the pressure coefficient i.e. C_P and it is zoomed in on the connection in Figure 11. The longitudinal distribution of the pressure force component i.e. ΔX_P is presented in Figure 12. Its integral value corresponds to the pressure resistance in the following:

$$R_P = -\int \frac{dX_P}{dx} dx \quad (2)$$

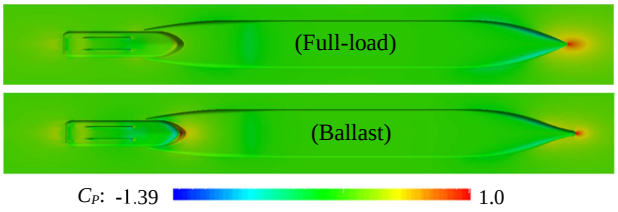

Figure 10: [Bottom view] Contours of the pressure coefficient around the P/B (above: Full-load / below: Ballast)

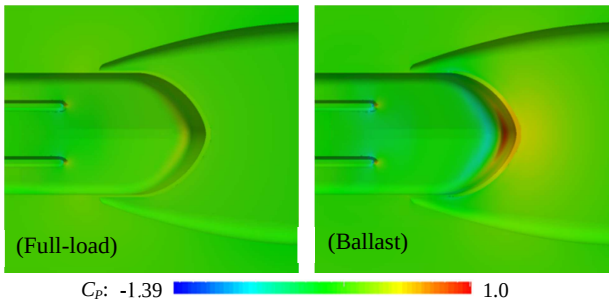

Figure 11: Enlarged bottom view of the contours of the pressure coefficient around the P/B (left: Full-load / right: Ballast)

From Figure 12, we see the significant change of ΔX_p occurs around the bow of the barge. The amount of change increases when the barge draft increases. It is because the significant stagnation due to the blunt shape of the barge occurs and results in the change of the pressure as shown in Figure 10. Meanwhile, as expected from the contours of the velocity, i.e., Figure 8, we see from Figure 11 that the positive pressure spreads over the pusher bow behind the ballast barge in contrast with when pushing the full-load barge. It is because the flow is stagnant there. Since this pressure field pushes the barge forward, and

JOMAse | Received: 12-October-2017 | Accepted: 30-November-2017 | [(49) 1: 1-7]
Published by International Society of Ocean, Mechanical and Aerospace Scientists and Engineers, www.isomase.org., ISSN: 2354-7065 & e-ISSN: 2527-6085

pushes the pusher backward, the pressure fluctuation drastically occurs in the case of P/B(Ballast) as shown in Figure 12.

As the result, although the pressure resistance of the barge of the P/B(Ballast) is smaller than the P/B(Full-load) (ref: blue bar of "B of P/B" in Figs. 5 and 6), that of the pusher is overwhelmingly larger. Thus, the total pressure resistance acting on the P/B results in similar regardless of the large difference of the barge displacement.

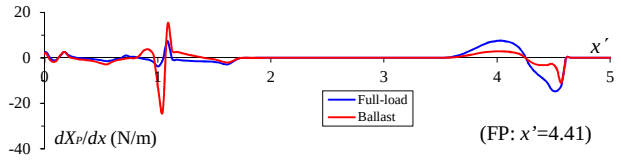

Figure 12: Longitudinal distribution of the pressure force component

5.0 INFLUENCE OF CLEARANCE ON RESISTANCE

5.1 Case study: No clearance

In order to sail in waves, a P/B commonly has a pivot (2-pin) to accept the relative pitching motion of the pusher to the barge, and there is a small clearance between the pusher and barge to prevent the bow of the pusher from hitting the stern of the barge. Meanwhile, such a discontinuous part (clearance) disturbs the smooth flow and generates vortices as presented in the previous chapter. It concerns us about the increase of the viscous pressure resistance. One idea to solve this problem is to fix the pusher to the barge completely by e.g. 3-pin supported rigid connection [8]. If so, the clearance designed for the relative pitching motion is not needed any more. From this viewpoint, the influence of the clearance on the resistance is discussed in this section.

We designed the new hull form of the P/B without the clearance by extending the bottom surface of the slope at the stern of the barge and covering the clearance. Figure 13 shows the results of the resistance. The contours of the velocity and pressure coefficient around the connection are presented in Figure 14 and Figure 15. As expected, we see the P/B with no clearance has the smaller resistance than the original case under the full-load condition: the reduction rate of the pressure resistance reaches about 12.3 % which results in the reduction of the total resistance i.e. about 3.7 %. Figure 14 is helpful to understand the phenomena in which the stream lines are continuously smooth along the bottom hull surface. Thus, it brings about the better resistance performance. On the other hand, the resistance of the P/B with no clearance increases more than the original case under the ballast condition: the increase rate of the total resistance reaches about 9.6 %, and we can see it is due to the increase of the pressure resistance. With focus on the right figure in Figure 11, the positive pressure is developed within the recess part of the original P/B under the ballast condition. It brings about the significant reduction of the pressure resistance of the barge, although the pressure resistance of the pusher increases. In the case of no clearance (ref: right figure in Fig.15), the positive pressure spread over the flat bottom surface of the barge around the connection cannot push the barge forward strongly, the pressure resistance of the pusher is dominant which results in the increase of the total resistance as unexpected.

5.2 Case study: A variety of clearance

It is interesting to investigate the influence of the clearance on the resistance systematically. Then, we assumed the several cases of the clearance between the pusher and barge and calculated the resistance in each of them. The result is compared in Figure 16 (Full-load) and Figure 17 (Ballast).

The total resistance increases with increase of the clearance. It is a common tendency for both full-load and ballast conditions. In the case of the ballast condition (ref: Fig.17), the propulsive pressure force (negative pressure resistance) acting on the barge decreases significantly with increase of the clearance. It is because the barge is difficult to receive the benefit from the positive pressure spread over the pusher bow. Meanwhile, regarding the full-load condition (ref: Fig.16), the pressure resistance acting on the pusher mainly increases as the clearance increases. It would be considered because the strength of the wake shed from the barge is weaken at the pusher position and the flow directly come into the pusher bow, the average flow velocity around the pusher becomes faster. In any case, the case of the smallest clearance i.e. 0.5 (m) shows the smallest resistance performance among these clearance cases.

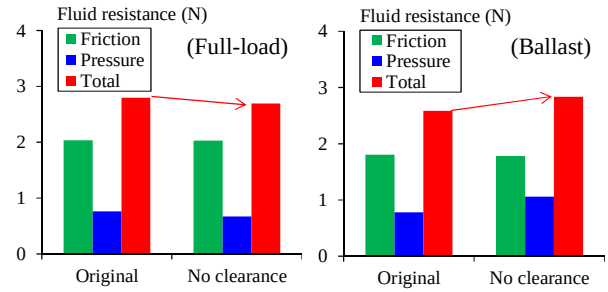

Figure 13: Comparison of the resistance between the original P/B and the P/B with no clearance at the connection (left: Full-load / right: Ballast)

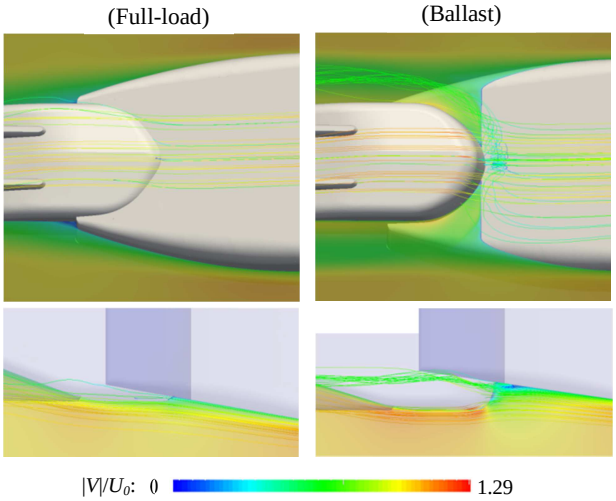

Figure 14: Comparison of the contours of the nondimensional flow velocity around the P/B with no clearance at the connection (left: Full- load / right: Ballast)

JOMAse | Received: 12-October-2017 | Accepted: 30-November-2017 | [(49) 1: 1-7]
Published by International Society of Ocean, Mechanical and Aerospace Scientists and Engineers, www.isomase.org., ISSN: 2354-7065 & e-ISSN: 2527-6085

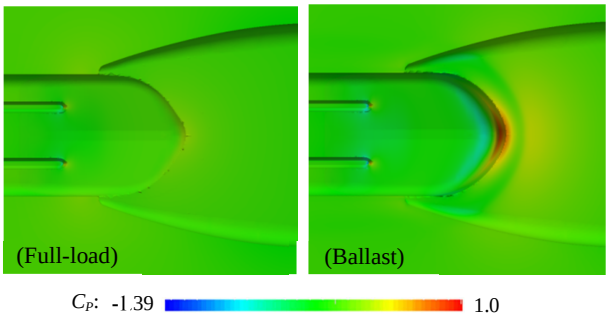

Figure 15: Comparison of the contours of the pressure coefficient around the P/B with no clearance at the connection (left: Full-load / right: Ballast)

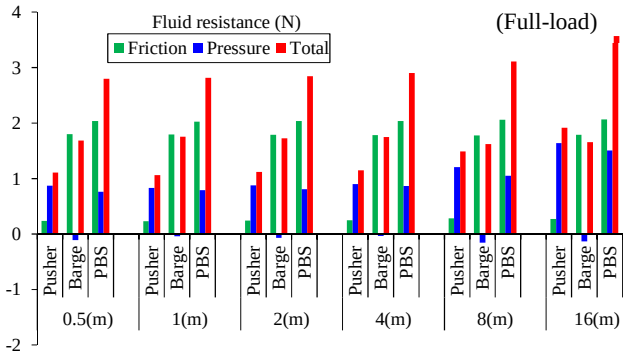

Figure 16: Comparison of the resistance of the P/B with a variety of clearances at the connection (Full-load)

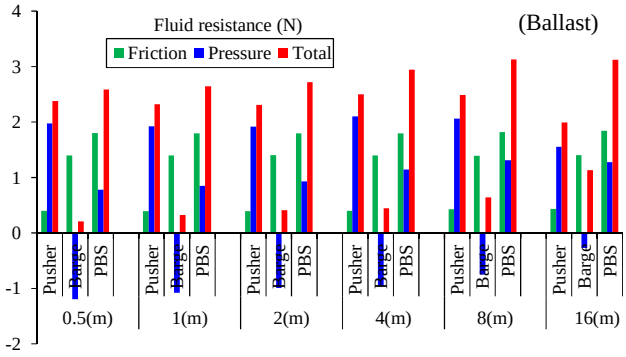

Figure 17: Comparison of the resistance of the P/B with a variety of clearances at the connection (Ballast)

6.0 CONCLUSION

Since a sea-going P/B competes against normal cargo ships at sea, the resistance performance of the P/B is more important than a river-going P/B. Therefore, in this study, a fundamental investigation was conducted based on CFD analysis, considering the two barge load conditions: full-load and ballast conditions. The mechanism of the resistance in each condition was discussed through visualization of the flow/pressure field. We found the unique characteristics of the resistance of the P/B were related to the strength of the interaction between the pusher and barge.

The influence of the clearance at the connection, which is required accept the relative pitching motion of the pusher to the barge in waves, was also studied. No clearance which means the pusher is completely fixed to the barge is effective to reduce the P/B under the full-load condition. However, it is not necessarily useful when pushing the ballast barge. That difference occurs due to the difference of the mechanism of the resistance according to barge load conditions.

ACKNOWLEDGEMENTS

The authors appreciate Mr. Yamaguchi and Mr. Sadakuni from Taisei Engineering Consultants, Inc. for providing the reference data of the P/B and useful advice. This study was supported by Grant-in-Aid for Scientific Research (C) of JSPS KAKENHI Grant Number 16K06906. The authors would like to express their gratitude to the grant-in-aid.

REFERENCE

1. National waterways foundation (2008). *Waterways: working for America*, (http://www.nationalwaterwaysfoundation.org/study/Work4America.pdf) (accessed to 2017-10-10)
2. Yasukawa H., Hirata N., Koh K. K., Krisana P. and Kose K. (2007). *Hydrodynamic force characteristics on maneuvering of pusher-barge systems*, Journal of the Japan Society of Naval Architects and Ocean Engineers, Vol. 5, pp. 133-142. (in Japanese)
3. Koh K. K., Yasukawa H., Hirata N. and Kose K. (2008). *Maneuvering simulations of pusher-barge systems*, Journal of Marine Science Technology, Vol.13, pp.117–126.
4. Hamaguchi T., Sano M. and Yasukawa H. (2016). *Maneuvering Simulation of Pusher-Barge Systems in Uniform River Flow*, Proc. of Ocean, Mechanical and Aerospace -Science and Engineering-, Terengganu, Malaysia, Vol.3 (Nov 2016), pp.242-253.
5. Maimun A., Priyanto A., Muhammad A. H., Scully C. C. and Awal Z. I. (2011). *Manoeuvring prediction of pusher barge in deep and shallow water*, Ocean Engineering, Vol.38, pp.1291-1299.
6. Sano M. and Hasegawa K. (2015). *A fundamental study on the ship handling simulation of tug-barge and pusher-barge systems for river service*, Proc. of International conference on ship and offshore technology - India2015 (ICSOT INDIA-2015), Kharagpur, India, pp.141-150.
7. Yamaguchi T. (1984). Twelve years' experience with articouple pusher-barge system, Proc. of the 8th international tug convention, Singapore, pp.211-226.

JOMAse | Received: 12-October-2017 | Accepted: 30-November-2017 | [(49) 1: 1-7]
Published by International Society of Ocean, Mechanical and Aerospace Scientists and Engineers, www.isomase.org., ISSN: 2354-7065 & e-ISSN: 2527-6085

8. Articouple and Triofix. Taisei Engineering Consultants, Inc. (http://www.articouple.com/), (accessed to 2017-10-10).
9. Yamaguchi T. (2013). *Chapter 4: Availability of pusher-barge system in Southeast Asian countries*, Document delivered in the informal workshop about pusher and barge system, Hiroshima. (in Japanese)
10. The open source CFD toolbox, OpenFOAM, (http://www.openfoam.com/), (accessed to 2017-10-10).

JOMAse | Received: 12-October-2017 | Accepted: 30-November-2017 | [(49) 1: 1-7]
Published by International Society of Ocean, Mechanical and Aerospace Scientists and Engineers, www.isomase.org., ISSN: 2354-7065 & e-ISSN: 2527-6085